

# Sub-gap kinetic inductance detector sensitive to 85 GHz radiation

F. Levy-Bertrand,<sup>1,\*</sup> A. Benoit,<sup>1</sup> O. Bourrion,<sup>2</sup> M. Calvo,<sup>1</sup> A. Catalano,<sup>2</sup> J. Goupy,<sup>1</sup>  
F. Valenti,<sup>3,4</sup> N. Maleeva,<sup>4</sup> L. Grünhaupt,<sup>4</sup> I. M. Pop,<sup>5,4</sup> and A. Monfardini<sup>1,†</sup>

<sup>1</sup>*Univ. Grenoble Alpes, CNRS, Grenoble INP, Institut Néel, 38000 Grenoble, France*

<sup>2</sup>*Laboratoire de Physique Subatomique et de Cosmologie, Université Grenoble Alpes,  
CNRS, 53 rue des Martyrs, 38026 Grenoble Cedex, France*

<sup>3</sup>*IPE, Karlsruhe Institute of Technology, 76344 Eggenstein-Leopoldshafen, Germany*

<sup>4</sup>*PHI, Karlsruhe Institute of Technology, 76131 Karlsruhe, Germany*

<sup>5</sup>*IQMT, Karlsruhe Institute of Technology, 76344 Eggenstein-Leopoldshafen, Germany*

We have fabricated an array of Sub-gap Kinetic Inductance Detectors (SKIDs) made of granular aluminum ( $T_c \sim 2$  K) sensitive in the 80-90 GHz frequency band and operating at 300 mK. We measured a noise equivalent power of  $1.3 \times 10^{-16}$  W/Hz<sup>0.5</sup> on average and  $2.6 \times 10^{-17}$  W/Hz<sup>0.5</sup> at best, for an illuminating power of 50 fW per pixel. Even though the circuit design of SKIDs is identical to that of the Kinetic Inductance Detectors (KIDs), the SKIDs operating principle is based on their sensitivity to sub-gap excitations. This detection scheme is advantageous because it avoids having to lower the operating temperature proportionally to the lowest detectable frequency. The SKIDs presented here are intrinsically selecting the 80-90 GHz frequency band, well below the superconducting spectral gap of the film, at approximately 180 GHz.

PACS numbers:

## I. INTRODUCTION

Terahertz (THz) electromagnetic waves are defined from 0.1 THz to 10 THz, corresponding to wavelengths from 3 mm down to 30  $\mu\text{m}^{1-3}$ . These waves are non-ionizing and can pass through wood, plastic, clothing and the atmosphere in a few frequencies bands (THz atmospheric transmission windows). Most molecules have vibration or rotation frequencies in the THz range, allowing spectroscopic identification<sup>4,5</sup>. These properties drive the development of THz imaging and THz spectroscopy for various potential applications such as security<sup>6</sup>, medical diagnostic<sup>7</sup>, quality control process and astrophysics research<sup>8,9</sup>. To better exploit these potential applications, two main research directions are being conducted: the development of sensitive detectors and the development of intense sources. The present work focuses on the investigation of a new kind of sensitive detector, the Sub-gap Kinetic Inductance Detector<sup>10</sup> (SKID), a particular implementation of the Kinetic Inductance Detector concept (KID)<sup>11-13</sup>.

KIDs are detectors used for millimeter wave observations in astrophysics<sup>14-17</sup> and for emerging security THz passive cameras<sup>18,19</sup>. They are planar resonant circuits made of superconductors deposited on an insulating substrate. They are usually cooled down to about 100 mK. The photon detection principle consists in monitoring the resonance frequency shift that is proportional to the incident power. Thanks to a straightforward fabrication process, an easy multiplexing technique and a compact design, KIDs are ideal to achieve large sensitive arrays with thousands of pixels, such as the ones currently installed in the NIKA2 millimetric camera of the IRAM 30 m telescope (Pico Veleta, Spain)<sup>20</sup>. The current NIKA2 KIDs arrays have a total of about 3000 KIDs of thin superconducting aluminum, operating at

150 mK and detecting frequencies in the 120-300 GHz band. Their noise equivalent power is of the order of  $10^{-17}$ W/Hz<sup>0.5</sup> to  $10^{-16}$ W/Hz<sup>0.5</sup> as required for ground-based observations.

The circuit design of SKIDs is identical to that of the Kinetic Inductance Detectors. The photon detection principle also consists in monitoring the resonance frequency shift that is proportional to the incident power. However, the mechanism giving rise to the frequency shift is different. For classic KIDs<sup>11</sup>, in order to generate a frequency shift the incident photon must carry an energy  $h\nu$  higher than or equal to the superconducting gap  $2\Delta$ . This gap is the minimum energy required to break the Cooper pairs forming the superfluid. Thus, for a given superconducting material, the smallest detectable frequency is  $\nu_{low} = 2\Delta/h$ . An associated constraint is that, in order to exclude temperature induced excitations, the operating temperature must be less than or equal to  $T \sim 2\Delta/(35k_B)$  where  $k_B$  is the Boltzmann constant<sup>34</sup>. In short, for classic KIDs, reducing the smallest detectable frequency requires a proportional reduction of the operating temperature. For detection at 80 GHz, an operating temperature lower than  $\sim 100$  mK would thus be needed. The working principle of SKIDs removes this constraint. For SKIDs<sup>10,21</sup>, the shift of the measured frequency is due to absorbed photons at a sub-gap excitation frequency. This mechanism is known as the cross-Kerr effect. It occurs because in superconducting thin films the superfluid density, and thus the kinetic inductance, depends on the current<sup>10,22,23</sup>, and the circulating current is increased by adding photons. Below the superconducting gap, adding photons is only possible if sub-gap excitations exist, otherwise the superconductor is a perfect mirror (the photons are reflected). Sub-gap excitations can be higher order of the fundamental resonance frequency<sup>10,24</sup> or phase and amplitude fluctuations

of the superconducting order parameter<sup>21</sup> (respectively Goldstone and Higgs modes). The higher is the cross-Kerr coefficient, the more sensitive is the SKID detector.

Here we report the performances of a Sub-gap Kinetic Inductance Detector array made of superconducting granular aluminum (grAl, see Fig. 1). The sensitivity of superconducting granular aluminium layer to sub-gap excitations has been evidenced in a previous study<sup>21</sup>. The intense sensitivity at about 85 GHz is interpreted as a divergence of the density of sub-gap modes at the two-dimensional plasma frequency<sup>24</sup>, explaining why the SKIDs are intrinsically selecting the 80-90 GHz frequency band. These SKIDs may provide a potential option for imaging at 85 GHz.

## II. EXPERIMENTAL

Figure 1 shows the design of a SKID array (top panel) and a schematic representation of the experimental set-up. The SKID array consists in twenty-two LC-resonators coupled to a feedline in a coplanar waveguide (CPW) configuration. The inductor  $L$ , the radiation sensitive element, is identical for all the resonators while the finger length of the capacitors  $C$  are adjusted to tune the resonant frequency  $f = 1/(2\pi\sqrt{LC})$  and achieve frequency multiplexing. The array is deposited on a  $330 \mu\text{m}$  thick sapphire substrate. The feedline and the ground plane are made of a 20 nm thick aluminum layer with a normal state resistivity of  $\sim 2 \mu\Omega\text{cm}$ , a critical temperature of  $\sim 1.4 \text{ K}$  and a superconducting gap  $2\Delta/h \sim 100 \text{ GHz}$ <sup>25</sup>. The resonators are made of a 20 nm thick granular aluminium<sup>26–30</sup> layer with a normal state resistivity of  $\sim 900 \mu\Omega\text{cm}$ , a critical temperature of  $\sim 2 \text{ K}$  and a superconducting gap  $2\Delta/h \sim 180 \text{ GHz}$ . The array is cooled at 300 mK in an optical dilution refrigerator. Photons illuminate the resonators from outside the cryostat through a series of optical filters. The filters configuration ensured that only photons with energy  $\nu < 110 \text{ GHz}$  reach the resonators. Nineteen out of twenty-two SKIDs were functional, with fundamental resonance frequencies ranging from 2.86 GHz to 3.79 GHz.

## III. RESULTS AND DISCUSSION

A standard protocol to quantify the efficiency of a photon detector is to evaluate its noise equivalent power<sup>10,25,31,32</sup> (NEP) which corresponds to the signal power producing a signal-to-noise ratio of one in a one Hertz output bandwidth. NEP is defined in this case as:

$$\text{NEP} = \frac{\Delta W_{\text{opt}} S_f}{\Delta f} \quad (1)$$

where  $W_{\text{opt}}$  is the optical load power per detector,  $\Delta f$  is the frequency shift of the resonance generated by the change of the optical load  $\Delta W_{\text{opt}}$  (the power to be de-

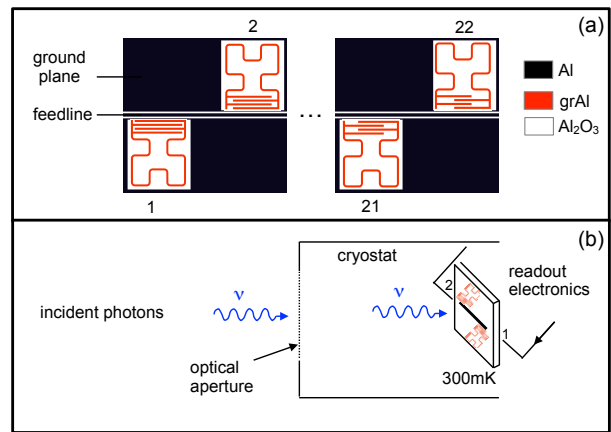


FIG. 1: **Sub-gap Kinetic Inductance Detectors design and experimental set-up.** (a) The SKIDs, in red, are planar resonators made out of superconducting granular aluminum (grAl). They consist in a Hilbert fractal inductor and a capacitive element that is adjusted to tune the resonant frequency. (b) Photons illuminate the resonators through optical apertures and filters of a dilution refrigerator operating at 300 mK. The resonance frequency shifts are monitored through the transmission coefficient  $S_{21}$  of the feedline.

tected), and  $S_f$  is the noise spectral density. The smaller the NEP, the more sensitive the detector.

Figure 2 displays the frequency shift of the resonance due to a change of the optical load. The figure shows the magnitude of the transmission coefficient  $|S_{21}|$  of the feedline for the best SKID (number #2) for two different incident optical powers. The resonance frequency shifts by almost 8 kHz when the temperature of the black body source is changed from 300 K to 60 K. The average frequency shift of the array is 8.5 kHz, with a standard deviation of 1.4 kHz.

The evaluation of the change of the optical load per detector,  $\Delta W_{\text{opt}}$ , is done using a three-dimension ray-tracing software where the inputs are the spectral luminance of the source (a black body source at 300 K and 60 K), the geometry of the cryostat (the apertures, the distances, the lenses curvatures and materials), the size of the detector ( $\sim 400 \times 400 \mu\text{m}^2$ ) and the spectral response of the detector. The spectral response of the detector can be over-estimated by taking into account all the frequencies up to the low pass filter cutoff frequency at 110 GHz, leading to  $\Delta W_{\text{opt}}^{0-110 \text{ GHz}} \sim 0.2 \text{ pW}$ . The spectral response can also be measured, as presented below, leading to a smaller, and more realistic estimation of the change of the optical load  $\Delta W_{\text{opt}}^{82-92 \text{ GHz}} \sim 0.05 \text{ pW}$ . This power corresponds to imaging at 85 GHz.

Figure 3 presents measurement of the spectral response of SKID number #2. The top panel shows the actual measurement: the frequency shift as a function of the optical path difference of a Martin-Puplett spectrometer<sup>33</sup>. The Martin-Puplett spectrometer is a Fourier Transform Spectrometer with a beamsplitter that consist in a grid

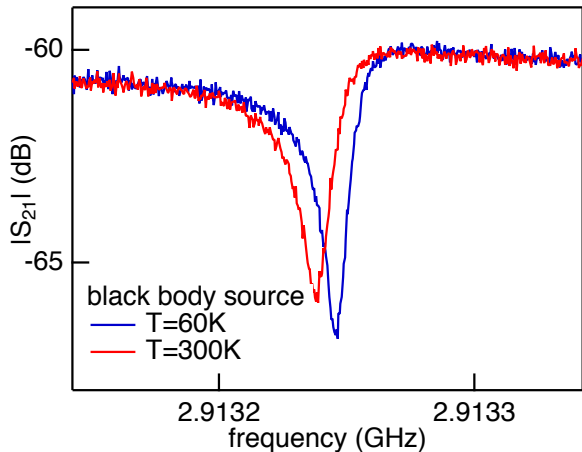


FIG. 2: **Photon detection demonstration for SKID #2.** The resonant frequency shifts down by 8 kHz when the temperature of a black body source illuminating the detector is increased from 60 K to 300 K. The black body spectrum is filtered by a low pass with a cut-off at 110 GHz.

of gold wires especially adapted for measurements in the 50 GHz - 3 THz range<sup>24,33</sup>. The radiation source is a broad band one that is split in two beams and recombined with an optical path difference that is varied thanks to a moving mirror. The intensity as a function of the optical path difference, the interferogram, is the sum of interference fringes of different wavelengths. The Fourier Transform of the interferogram, the spectrum, is the intensity as a function of the incoming light wavelength. For our measurements, we proceed to a lock-in detection by modulating the incoming broad band source between a black-body source at nitrogen temperature (77 K) and one at room temperature. The interferogram of the SKID number #2 (top panel) is almost a pure sinusoid with a few beating frequencies. The corresponding spectrum (the bottom panel) shows a maximum absorption at 86 GHz. The spectral response of the other SKIDs is similar: almost pure sinusoidal interferograms and spectra with a dominating absorption between 80 GHz to 90 GHz. The SKIDs made out of granular aluminum with a normal state resistivity of  $\sim 900 \mu\Omega\cdot\text{cm}$  are thus intrinsically selecting the 80-90 GHz frequency band with a low pass filter of 110 GHz to suppress the above-gap (standard KID) optical response.

Figure 4 shows the noise spectral density (NSD) of SKID number #2. Under a constant optical load, the variation of the resonance frequency of each SKID has been recorded over time and a Fourier Transform has been applied to get the NSD. At 10Hz, the NSD of SKID number #2 is  $N_f \sim 4 \text{ Hz}/\text{Hz}^{0.5}$ . At 10 Hz, the average NSD of the array is  $28 \text{ Hz}/\text{Hz}^{0.5}$  with a standard deviation of  $17 \text{ Hz}/\text{Hz}^{0.5}$ . The uniformity of the array has to be improved. In particular, the response seems homogeneous, but the noise is very variable. This last point needs

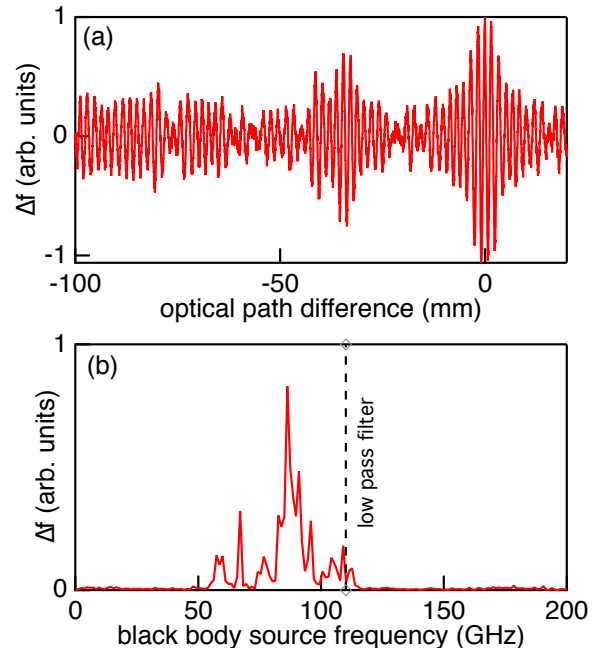


FIG. 3: **Spectral response of SKID #2.** (a) Frequency shift as a function of the optical path difference of a Martin-Puplett spectrometer. (b) Frequency shift as a function of incident photon frequency. Fourier Transform of the top panel response.

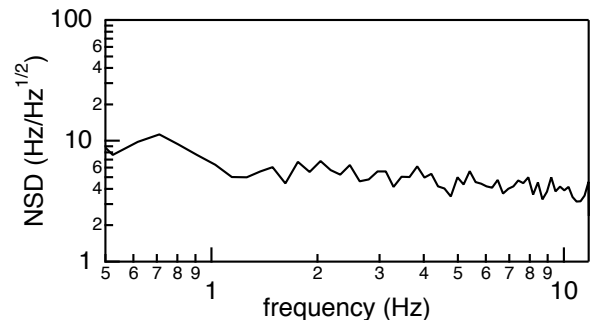


FIG. 4: **Noise spectral density (NSD) of SKID #2.**

to be understood. Optimization of the readout power per SKID may help.

Figure 5 presents the evaluation of the noise equivalent power of our detectors with equation (1) using the smallest value of the optical load variation. For the best detector, SKID number #2, we get a NEP of  $2.6 \times 10^{-17} \text{ W}/\text{Hz}^{0.5}$ , comparable to the result obtained on KIDs made of Ti-Al bilayer operating at 100 mK for a 80-120 GHz frequency band<sup>25</sup>. The average NEP of the SKIDs array is  $1.3 \times 10^{-16} \text{ W}/\text{Hz}^{0.5}$  for an operating temperature of 300 mK and a 80-90 GHz frequency band.

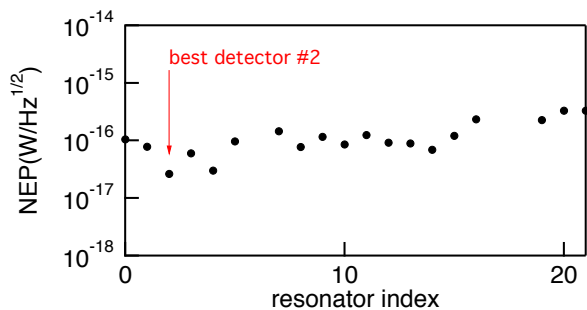


FIG. 5: Noise equivalent power of a SKIDs array for a 80-90 GHz frequency range. The SKIDs are identified by their index from 0 to 21, see figure 1a (19 out of 22 were functional resonators).

#### IV. CONCLUSION

The presented grAl SKID are potentially of interest for imaging applications in the 80-90 GHz band. Indeed, the upscaling of our array to a larger one is technically possible. The readout electronics is already available to address up to 400 detectors per feedline. Also, the base temperature requirement of 300 mK, instead of 100 mK, simplifies the cryogenic setup, although the need of sub-K temperatures still implies the use of relatively complex instrumentation. The intrinsic frequency selectivity of these detectors may be used as a natural band-pass

filter. However, we still have not implemented a mechanism to tune the absorption band. Further investigation may increase the required minimum operating temperature by unveiling other superconducting materials with collective sub-gap modes and higher critical temperature. Beside, THz-spectroscopy on chip may be envisioned if a solution is found to tune in situ the frequencies of the sub-gap modes. Possible options include, for example, the use of applied magnetic fields and/or DC currents. Magnetic fields and DC currents reduce the superfluid density. The energy of the sub-gap superconducting excitations (and therefore their frequencies) will be varied in turn.

#### Acknowledgments

We acknowledge the contributions of the Cryogenics and Electronics groups at Institut Néel and LPSC. This work has been partially supported by the French National Research Agency through Grant No. ANR-16-CE30-0019 ELODIS2 and by the LabEx FOCUS through Grant No. ANR-11-LABX-0013. F.L-B acknowledges financial support from the CNRS through a grant *Défi Instrumentation aux limites 2018*. F.V., N.M., L.G. and I.M.P acknowledge the Alexander von Humboldt Foundation in the framework of a Sofja Kovalevskaja award endowed by the German Federal Ministry of Education and Research.

\* Electronic address: florence.levy-bertrand@neel.cnrs.fr

† Electronic address: alessandro.monfardini@neel.cnrs.fr

<sup>1</sup> M. Tonouchi, “Cutting-edge thz technology,” *Nat. Photonics*, vol. 1, pp. 97–105, 02 2007.

<sup>2</sup> A. Rogalski and F. Sizov, “Terahertz detectors and focal plane arrays,” *Opto-Electronics Review*, vol. 19, no. 3, pp. 346 – 404, 2011.

<sup>3</sup> S. S. Dhillon, M. S. Vitiello, E. H. Linfield, A. G. Davies, M. C. Hoffmann, J. Booske, C. Paoloni, M. Gensch, P. Weightman, G. P. Williams, E. Castro-Camus, D. R. S. Cumming, F. Simoens, I. Escorcia-Carranza, J. Grant, S. Lucyszyn, M. Kuwata-Gonokami, K. Konishi, M. Koch, C. A. Schmuttenmaer, T. L. Cocker, R. Huber, A. G. Markelz, Z. D. Taylor, V. P. Wallace, J. A. Zeitler, J. Sibik, T. M. Korter, B. Ellison, S. Rea, P. Goldsmith, K. B. Cooper, R. Appleby, D. Pardo, P. G. Huggard, V. Krozer, H. Shams, M. Fice, C. Renaud, A. Seeds, A. Stöhr, M. Nafataly, N. Ridler, R. Clarke, J. E. Cunningham, and M. B. Johnston, “The 2017 terahertz science and technology roadmap,” *Journal of Physics D: Applied Physics*, vol. 50, p. 043001, Jan. 2017.

<sup>4</sup> T. Encrenaz, B. Bézard, J. Crovisier, A. Coustenis, E. Lellouch, S. Gulkis, and S. Atreya, “Detectability of molecular species in planetary and satellite atmospheres from their rotational transitions,” *Planetary and Space Science*, vol. 43, pp. 1485–1516, Dec. 1995.

<sup>5</sup> T. G. Phillips and J. Keene, “Submillimeter astronomy (heterodyne spectroscopy),” *Proceedings of the IEEE*, vol. 80, no. 11, pp. 1662–1678, 1992.

<sup>6</sup> D. Mittleman, *Sensing with Terahertz Radiation*. Springer, Berlin, Feb. 2013.

<sup>7</sup> P. H. Siegel, “Terahertz technology in biology and medicine,” *IEEE Transactions on Microwave Theory and Techniques*, vol. 52, no. 10, pp. 2438–2447, 2004.

<sup>8</sup> A. Monfardini, R. Adam, A. Adane, P. Ade, P. André, A. Beelen, B. Belier, A. Benoit, A. Bideaud, N. Bilot, O. Bourrion, M. Calvo, A. Catalano, G. Coiffard, B. Comis, A. D’Addabbo, F.-X. Désert, S. Doyle, J. Goupy, C. Kramer, S. Leclercq, J. Macias-Perez, J. Martino, P. Mausekopf, F. Mayet, F. Pajot, E. Pascale, N. Ponthieu, V. Revéret, L. Rodriguez, G. Savini, K. Schuster, A. Sievers, C. Tucker, and R. Zylka, “Latest NIKA Results and the NIKA-2 Project,” *Journal of Low Temperature Physics*, vol. 176, pp. 787–795, Sept. 2014.

<sup>9</sup> J. Schlaerth, A. Vayonakis, P. Day, J. Glenn, J. Gao, S. Golwala, S. Kumar, H. LeDuc, B. Mazin, J. Vaillancourt, and J. Zmuidzinas, “A Millimeter and Submillimeter Kinetic Inductance Detector Camera,” *Journal of Low Temperature Physics*, vol. 151, pp. 684–689, May 2008.

<sup>10</sup> O. Dupré, A. Benoît, M. Calvo, A. Catalano, J. Goupy, C. Hoarau, T. Klein, K. L. Calvez, B. Sacépé, A. Monfardini, and F. Levy-Bertrand, “Tunable sub-gap radiation

- detection with superconducting resonators,” *Superconductor Science and Technology*, vol. 30, p. 045007, Feb. 2017.
- 11 P. K. Day, H. G. LeDuc, B. A. Mazin, A. Vayonakis, and J. Zmuidzinas, “A broadband superconducting detector suitable for use in large arrays,” *Nature*, vol. 425, pp. 817–821, Oct. 2003.
  - 12 S. Doyle, P. Mauskopf, J. Naylor, A. Porch, and C. Dunscombe, “Lumped element kinetic inductance detectors,” *Journal of Low Temperature Physics*, vol. 151, pp. 530–536, Jan. 2008.
  - 13 H. McCarrick, D. Flanigan, G. Jones, B. R. Johnson, P. Ade, D. Araujo, K. Bradford, R. Cantor, G. Che, P. Day, S. Doyle, H. Leduc, M. Limon, V. Luu, P. Mauskopf, A. Miller, T. Mroczkowski, C. Tucker, and J. Zmuidzinas, “Horn-coupled, commercially-fabricated aluminum lumped-element kinetic inductance detectors for millimeter wavelengths,” *Review of Scientific Instruments*, vol. 85, p. 123117, Dec. 2014.
  - 14 A. Patel, A.-D. Brown, W.-T. Hsieh, T. Stevenson, S. H. Moseley, K. U-yen, N. Ehsan, E. Barrentine, G. Manos, and E. J. Wollack, “Fabrication of MKIDS for the MicroSpec Spectrometer,” *IEEE Transactions on Applied Superconductivity*, vol. 23, pp. 2400404–2400404, June 2013. Conference Name: IEEE Transactions on Applied Superconductivity.
  - 15 T. Matsumura, Y. Akiba, J. Borrill, Y. Chinone, M. Dobbs, H. Fuke, A. Ghribi, M. Hasegawa, K. Hattori, M. Hattori, M. Hazumi, W. Holzapfel, Y. Inoue, K. Ishidoshiro, H. Ishino, H. Ishitsuka, K. Karatsu, N. Katayama, I. Kawano, A. Kibayashi, Y. Kibe, K. Kimura, N. Kimura, K. Koga, M. Kozu, E. Komatsu, A. Lee, H. Matsuhara, S. Mima, K. Mitsuda, K. Mizukami, H. Morii, T. Morishima, S. Murayama, M. Nagai, R. Nagata, S. Nakamura, M. Naruse, K. Natsume, T. Nishibori, H. Nishino, A. Noda, T. Noguchi, H. Ogawa, S. Oguri, I. Ohta, C. Otani, P. Richards, S. Sakai, N. Sato, Y. Sato, Y. Sekimoto, A. Shimizu, K. Shinozaki, H. Sugita, T. Suzuki, A. Suzuki, O. Tajima, S. Takada, S. Takakura, Y. Takei, T. Tomaru, Y. Uzawa, T. Wada, H. Watanabe, M. Yoshida, N. Yamasaki, T. Yoshida, and K. Yotsumoto, “Mission Design of LiteBIRD,” *Journal of Low Temperature Physics*, vol. 176, pp. 733–740, Sept. 2014.
  - 16 M. Griffin, J. Baselmans, A. Baryshev, S. Doyle, M. Grim, P. Hargrave, T. Klapwijk, J. Martin-Pintado, A. Monfardini, A. Neto, H. Steenbeek, I. Walker, K. Wood, A. D’Addabbo, P. Barry, A. Bideaud, B. Blázquez, J. Bueno, M. Calvo, J.-L. Costa-Kramer, L. Ferrari, A. Gómez-Gutiérrez, J. Goupy, N. Llombart, and S. Yates, “SPACEKIDS: kinetic inductance detectors for space applications,” in *Millimeter, Submillimeter, and Far-Infrared Detectors and Instrumentation for Astronomy VIII*, vol. 9914, p. 991407, International Society for Optics and Photonics, July 2016.
  - 17 J. Baselmans, J. Bueno, O. Yurduseven, S. Yates, N. Llombart, V. Murugesan, D. J. Thoen, A. Baryshev, and A. Neto, “Performance of a 961 pixel kinetic inductance detector system for future space borne observatories,” in *2016 41st International Conference on Infrared, Millimeter, and Terahertz waves (IRMMW-THz)*, pp. 1–1, Sept. 2016. ISSN: 2162-2035.
  - 18 S. Rowe, E. Pascale, S. Doyle, C. Dunscombe, P. Hargrave, A. Papageorgio, K. Wood, P. A. R. Ade, P. Barry, A. Bideaud, T. Brien, C. Dodd, W. Grainger, J. House, P. Mauskopf, P. Moseley, L. Spencer, R. Sudiwala, C. Tucker, and I. Walker, “A passive terahertz video camera based on lumped element kinetic inductance detectors,” *Review of Scientific Instruments*, vol. 87, p. 033105, Mar. 2016. Publisher: American Institute of Physics.
  - 19 “<https://sequestim.com>.”
  - 20 Adam, R., Adane, A., Ade, P. A. R., André, P., Andrianasolo, A., Aussel, H., Beelen, A., Benoît, A., Bideaud, A., Billot, N., Bourrion, O., Bracco, A., Calvo, M., Catalano, A., Coiffard, G., Comis, B., De Petris, M., Désert, F.-X., Doyle, S., Driessen, E. F. C., Evans, R., Goupy, J., Kramer, C., Lagache, G., Leclercq, S., Leggeri, J.-P., Lestrade, J.-F., Macías-Pérez, J. F., Mauskopf, P., Mayet, F., Maury, A., Monfardini, A., Navarro, S., Pascale, E., Perotto, L., Pisano, G., Ponthieu, N., Revéret, V., Rigby, A., Ritacco, A., Romero, C., Roussel, H., Ruppín, F., Schuster, K., Sievers, A., Triqueneaux, S., Tucker, C., and Zylka, R., “The nika2 large-field-of-view millimetre continuum camera for the 30 m iram telescope,” *A&A*, vol. 609, p. A115, 2018.
  - 21 F. Levy-Bertrand, T. Klein, T. Grenet, O. Dupré, A. Benoît, A. Bideaud, O. Bourrion, M. Calvo, A. Catalano, A. Gomez, J. Goupy, L. Grünhaupt, U. v. Luepke, N. Maleeva, F. Valenti, I. M. Pop, and A. Monfardini, “Electrodynamics of granular aluminum from superconductor to insulator: Observation of collective superconducting modes,” *Physical Review B*, vol. 99, p. 094506, Mar. 2019.
  - 22 P. G. D. Gennes, *Superconductivity Of Metals And Alloys*. chapter 6.5.
  - 23 L. J. Swenson, P. K. Day, B. H. Eom, H. G. Leduc, N. Llombart, C. M. McKenney, O. Noroozian, and J. Zmuidzinas, “Operation of a titanium nitride superconducting microresonator detector in the nonlinear regime,” *Journal of Applied Physics*, vol. 113, p. 104501, Mar. 2013. Publisher: American Institute of Physics.
  - 24 N. Maleeva, L. Grünhaupt, T. Klein, F. Levy-Bertrand, O. Dupre, M. Calvo, F. Valenti, P. Winkel, F. Friedrich, W. Wernsdorfer, A. V. Ustinov, H. Rotzinger, A. Monfardini, M. V. Fistul, and I. M. Pop, “Circuit quantum electrodynamics of granular aluminum resonators,” *Nature Communications*, vol. 9, Sept. 2018.
  - 25 A. Catalano, J. Goupy, H. le Sueur, A. Benoit, O. Bourrion, M. Calvo, A. D’addabbo, L. Dumoulin, F. Levy-Bertrand, J. Macías-Pérez, S. Marnieros, N. Ponthieu, and A. Monfardini, “Bi-layer kinetic inductance detectors for space observations between 80–120 GHz,” *Astronomy & Astrophysics*, vol. 580, p. A15, July 2015.
  - 26 R. W. Cohen and B. Abeles, “Superconductivity in Granular Aluminum Films,” *Physical Review*, vol. 168, pp. 444–450, Apr. 1968. Publisher: American Physical Society.
  - 27 R. H. Parmenter, “Isospin Formulation of the Theory of a Granular Superconductor,” *Physical Review*, vol. 154, pp. 353–368, Feb. 1967. Publisher: American Physical Society.
  - 28 G. Deutscher, H. Fenichel, M. Gershenson, E. Grünbaum, and Z. Ovadyahu, “Transition to zero dimensionality in granular aluminum superconducting films,” *Journal of Low Temperature Physics*, vol. 10, pp. 231–243, Jan. 1973.
  - 29 R. C. Dynes and J. P. Garno, “Metal-Insulator Transition in Granular Aluminum,” *Physical Review Letters*, vol. 46, pp. 137–140, Jan. 1981. Publisher: American Physical Society.
  - 30 U. S. Pracht, N. Bachar, L. Benfatto, G. Deutscher, E. Farber, M. Dressel, and M. Scheffler, “Enhanced Cooper pair-

ing versus suppressed phase coherence shaping the superconducting dome in coupled aluminum nanograins,” *Physical Review B*, vol. 93, p. 100503(R), Mar. 2016. Publisher: American Physical Society.

- <sup>31</sup> A. Catalano, A. Bideaud, O. Bourrion, M. Calvo, A. Fasano, J. Goupy, F. Levy-Bertrand, J. F. Macias-Pérez, N. Ponthieu, Q. Y. Tang, and A. Monfardini, “Lekid sensitivity for space applications between 80 and 600 ghz,” 2020.
- <sup>32</sup> F. Valenti, F. Henriques, G. Catelani, N. Maleeva, L. Grünhaupt, U. von Lüpke, S. T. Skacel, P. Winkel, A. Bilmes, A. V. Ustinov, J. Goupy, M. Calvo, A. Benoît, F. Levy-Bertrand, A. Monfardini, and I. M. Pop, “Interplay between kinetic inductance, nonlinearity, and quasiparticle dynamics in granular aluminum microwave kinetic inductance detectors,” *Physical Review Applied*, vol. 11, p. 054087, May 2019.
- <sup>33</sup> D. Martin and E. Pulett, “Polarised interferometric spectrometry for the millimetre and submillimetre spectrum,” *Infrared Physics*, vol. 10, pp. 105–109, June 1970.
- <sup>34</sup>  $T \sim T_c/10$  and  $2\Delta = 3.52k_B T_c$  where  $T_c$  is the superconducting critical temperature